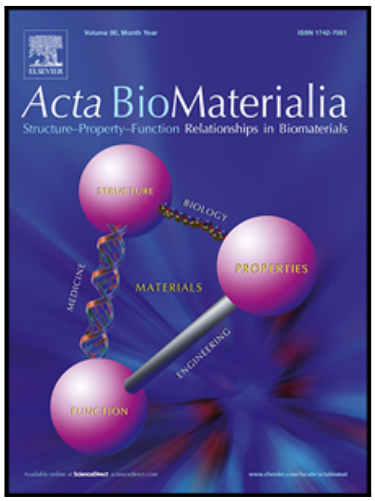

The Bone Morphogenetic Protein 2 Analogue L51P Enhances Spinal Fusion in Combination with BMP2 in an In Vivo Rat Tail Model

Benjamin Gantenbein , Katharina A.C. Oswald , Georg F. Erbach , Andreas S. Croft , Paola Bermudez-Lekerika , Franziska Strunz , Sebastian F. Bigdon , Christoph E. Albers

PII: S1742-7061(24)00050-3
DOI: https://doi.org/10.1016/j.actbio.2024.01.039
Reference: ACTBIO 9166

To appear in: *Acta Biomaterialia*

Received date: 27 July 2023
Revised date: 31 December 2023
Accepted date: 24 January 2024

Please cite this article as: Benjamin Gantenbein , Katharina A.C. Oswald , Georg F. Erbach , Andreas S. Croft , Paola Bermudez-Lekerika , Franziska Strunz , Sebastian F. Bigdon , Christoph E. Albers , The Bone Morphogenetic Protein 2 Analogue L51P Enhances Spinal Fusion in Combination with BMP2 in an In Vivo Rat Tail Model, *Acta Biomaterialia* (2024), doi: https://doi.org/10.1016/j.actbio.2024.01.039

The Bone Morphogenetic Protein 2 Analogue L51P Enhances Spinal Fusion in Combination with BMP2 in an *In Vivo* Rat Tail Model

Benjamin Gantenbein [1,2*], Katharina A. C. Oswald [2], Georg F. Erbach [2], Andreas S. Croft [1,3], Paola Bermudez-Lekerika [1,3], Franziska Strunz [1,3], Sebastian F. Bigdon [2] Christoph E. Albers [2]

Author's Affiliations

[1] Tissue Engineering for Orthopaedic & Mechanobiology, Bone & Joint Program, Department for BioMedical Research (DBMR), Medical Faculty, University of Bern, Bern, Switzerland.

[2] Department of Orthopaedic Surgery and Traumatology, Inselspital, Bern University Hospital, Medical Faculty, University of Bern, Bern, Switzerland

[3] Graduate School for Cellular and Biomedical Sciences (GCB), University of Bern, Bern, Switzerland

***Corresponding author:**
Benjamin Gantenbein - Tissue Engineering for Orthopaedics & Mechanobiology (TOM), Bone & Joint Program, Department for BioMedical Research (DBMR), Medical Faculty, University of Bern, Murtenstrasse 35, CH-3008 Bern, Switzerland.
Email: benjamin.gantenbein@unibe.ch
Tel: +41 31 632 88 15

To: **Acta Biomaterialia**

Keywords: spinal fusion, osteosynthesis, bone morphogenic protein 2, L51P BMP2 analogue, Wistar rat model of the elderly, β tricalcium phosphate

Abstract

Bone morphogenic protein 2 (BMP2) is known to induce osteogenesis and is applied clinically to enhance spinal fusion despite adverse effects. BMP2 needs to be used in high doses to be effective due to the presence of BMP2 inhibitors. L51P is a BMP2 analogue that acts by inhibition of BMP2 inhibitors. Here, we hypothesized that mixtures of BMP2 and L51P could achieve better spinal fusion outcomes regarding ossification. To test whether mixtures of both cytokines are sufficient to improve ossification, 45 elderly Wistar rats (of which 21 were males) were assigned to seven experimental groups, all which received spinal fusion surgery, including discectomy at the caudal 4-5 level using an external fixator and a porous β-tricalcium phosphate (βTCP) carrier. These βTCP carriers were coated with varying concentrations of BMP2 and L51P. X-rays were taken immediately after surgery and again six and twelve weeks post-operatively. Histological sections and µCT were analyzed after twelve weeks. Spinal fusion was assessed using X-ray, µCT and histology according to the Bridwell scale by voxel-based quantification and a semi-quantitative histological score, respectively.

The results were congruent across modalities and revealed high ossification for high-dose BMP2 (10 µg), while PBS induced no ossification. Low-dose BMP2 (1 µg) or 10 µg L51P alone did not induce relevant bone formation. However, all combinations of low-dose BMP2 with L51P (1 µg + 1/5/10 µg) were able to induce similar ossificationas high-dose BMP2. These results are of high clinical relevance, as they indicate L51P is sufficient to increase the efficacy of BMP2 and thus lower the required dose for spinal fusion.

1. Introduction

Low back pain (LBP) is the number one cause of disability worldwide, and 200 million more patients (currently ~600 million) are expected to suffer from LBP in the next 50 years [1]. Intervertebral disc (IVD) degeneration, a common cause of LBP, generates tremendous social health costs of up to 5% of the gross domestic product (GDP) of European countries [2-4]. However, LBP caused by disc degeneration or segmental instability can be treated with spinal fusion [5-7]. Spinal fusion is one of the most frequently performed surgical interventions in the spine [8,9]. Annually, over two million surgeries are performed worldwide [10]. The objective is to join one or more functional segments of the spine, eliminating motion between the segments and increasing stability [8,9,11-13]. However, failure of spinal fusion can lead to pseudoarthrosis, resulting in persistent instability and pain [14].

Urist first described bone morphogenic protein 2 (BMP2) as osteo-inductive in 1965 [15]. BMP2, BMP6, and BMP7 are frequently employed to improve osteo-inductivity, promote spinal fusion, and decrease the risk of pseudoarthrosis [16-20]. For example, BMP6 was used for spinal fusion applications and considered to be more resistant to Noggin (a prominent BMP inhibitor) inhibition [19,20]. BMPs are a complex family of cytokines with complex pathways and multiple BMP inhibitors have been described such as inhibitors of the differential screening-selected gene aberrative in neuroblastoma (DAN) family, the Chordin family (e.g., Chordin and Noggin), and Folllistatin, and Twisted Gastrulation have been recently discussed in detail [18].

Despite the use of these BMPs, failure of osseous fusion was reported in 5- 35.5% of surgeries, requiring revision surgery in up to 23.6% cases [5,7,21]. Lack of BMP efficacy could be due to the presence of BMP antagonists in the disc niche [22,23]. Moreover, an increasing body of evidence suggests that BMP use in pharmacological doses may be associated with significant adverse events, e.g., ectoptic ossification and development of cancer [24-29].

Prior *in vitro* data revealed that IVD cells exert inhibitory effects on the osteogenic differentiation of mesenchymal stem cells (MSCs) [23,30]. Similar effects of IVD cells could be shown on primary osteoblasts from patients [31]. Additionally, clinical trials revealed decreased fusion rates after incomplete removal of IVD cells [22,32,33]. Thus, endogenous BMP inhibitors, like Gremlin, Noggin, Chordin and Follistatin, of these cells might play a crucial role in preventing proper fusion [18]. Accordingly, the hypothesis of this study was

that blocking the inhibitory effects of BMP antagonists secreted by IVD cells would be sufficient to increase bone formation while reducing the dose of BMP2 currently used for spinal fusion. To achieve this, we aimed to antagonize the inhibition of bone formation by applying the BMP2 variant L51P in an *in vivo* rat model.

L51P has been previously shown to promote differentiation exclusively through inhibiting BMP2 antagonists [34]. For example, this has been demonstrated in an *in-vivo* critical bone size defect model in femurs of C57Bl/6J mice [34,35]. Thus, previous work on bone fracture healing in mice revealed L51P as a valid BMP2 analogue that is capable of inducing bone formation [35-38]. L51Pmost likely acts through competitive blocking of BMP inhibitors, such as Noggin, Chordin or Gremlin [36,38,39]. Further, *in-vitro* experiments confirmed that the inhibitory effects of IVD cells on osteoblast differentiation could be successfully reversed by adding L51P [30,31].

Improving the success of spinal fusion is key to reduce post-operative complications and the need for revision surgery and to lower the associated health costs [2,40]. Elucidating how BMP-signalling differs at the transitions between IVD, cartilage, and bone tissue could be crucial in making spinal fusion more effective. Using inhibitors to block BMP antagonists has the potential to improve patient outcome through enhanced spinal fusion rates and a reduced threshold of therapeutic BMP concentrations.

Here, we aimed to show an improved spinal fusion outcome by administrating a ceramic biomaterial combined with BMP2, the BMP2 analogue L51P and/or a combination of BMP2 and L51P. The hypothesis was that the addition L51P to BMP2 treatment is sufficient to decrease the concentration of BMP2 necessary to achieve spinal fusion. Male and female aged rats of approximately 12 months old were used and underwent inter-somatic spinal fusion of the rat tail with segmental fixation using an external ring fixator (Ex-Fix) [41].

2. Materials and Methods

2.1. Animals

The Wistar rats were either bought from Charles River Laboratories (Research Models and Services Germany GmbH, Sulzfeld, Germany) or were obtained (six rats) from the centralized animal facility (CAF, Medical Faculty, University of Bern, Switzerland). The animals were all checked for health issues and were provided with an ISO-certified health

report. Animals were kept for at least seven days prior to the experiment for adaptation in the professional animal facility with *ad libitum* food and in standardized conditions.

2.2. Animal experimental procedures

All animal experiments were carried out considering the ARRIVE guidelines and were carried out under the EU Directive 2010/63/EU for animal experiments. Permission for all described surgical procedures and applied drugs was obtained from the Swiss authorities of the canton of Bern (animal permit BE32/19). Elderly rats were used to best match the target patient population for treatment. In humans non-successful spinal fusion affects mostly the population > 70 years of age [2,7,42]. Rats at the age of 12-18 months correspond to this age in humans [41,43,44], and thus rats of this age group were used in this study. The experimental procedure described here has been published as a standard operational protocol (SOP) [45]. The current complete study design is illustrated in Figure 1. It comprised a double-blinded randomized design and included elderly Wistar rats (21 males, mean body weight 533.1 ± 148.8 g, mean ± SD, and 24 females, mean body weight 400.7 ± 52.7 g, respectively). The mean age of the rats was about 12 months to simulate the elderly population in humans [43,44]. For brevity, the protocol is recapitulated below. Animals were randomly assigned to seven experimental groups, which consisted of phosphate-buffered-saline (PBS) as material control, a "low-dose" (1µg) and a "high-dose" of (10µg) BMP2, a "high-dose" of the BMP2 analogue L51P (10µg), 1µg BMP2 and adding increasing doses of L51P, i.e., 1,5, or 10 µg (see figure 1 and Table 1).

2.3. Preparation of cytokine-coated βTCP

The βTCP was produced at RMS foundation according to previously described protocols [35,37,38,46]. The cytokines BMP2 and L51P were obtained by Prof. Dr. em. Walter Sebald, University of Heidelberg, Germany. These were produced by over-expression in *Escherichia coli* and subsequent purification from extrusion bodies as described previously [47,48] and were stored as lyophilized powder at -80°C prior to usage [34,37,38]. Predefined amounts of BMP2 and L51P (Table 1) were dissolved in 25 µl of deionized water and adsorbed to beta-tricalcium phosphate (βTCP) carriers according to an established protocol under sterile conditions (see video of [45]). The βTCP was of the same quality and production (RMS

foundation, Bettlach, Switzerland) as previously described, with a porosity of about 75% [35,46]. This βTCP was used because previous studies performed by our team showed convincing results in adult mice and fracture models [35,49]. The wetted ceramics were then air-dried overnight and implanted into the disc space after removal of the disc. The growth factor release of the βTCP carriers has already been studied and characterized in detail [35,46,50]. Eighty percent of the bound cytokine was "burst-released" after 4 days *in-vitro* in presence or absence of mouse calvaria osteoblasts [35,46].

2.4. Anaesthesia

Rats were anaesthetized with a balanced anaesthetic protocol (Fentanyl 0.005 mg/kg+ Medetomidine 0.15 mg/kg + Midazolam 2 mg/kg, all three from Sintetica S.A., Mendrisio, Switzerland, mixed in the same syringe and administered subcutaneously (s.c.). After s.c. injection of the anaesthetic mix, the rats were placed in a clean box and O_2 was provided until loss of consciousness (5-10 min). A surgical plane was granted for 45 min; 100% O_2 was provided via facemask throughout the surgery. If anaesthesia had to be prolonged after 45 min, it was continued with isoflurane (1.0- 2.0% titrated to effect in 100% O_2), allowing for adequate depth of anaesthesia.

With a mechanistic and balanced approach, intra and post-operative analgesia was provided by the epidural administration of 0.1 mL ropivacaine 0.5% between the vertebrae Cd1 and Cd2. Analgesia was calculated to last for about 3h. At the end of surgery, anesthesia was reversed with a mix of Buprenorphine 0.05 mg/kg (Streuli Pharma SA, Uznach, Switzerland) and Atipamezol 0.75 mg/kg (Orion Corporation, Espoo, Finland) and Flumazenil 0.2 mg/kg s.c. (CPS Cito Pharma Services GmbH, Uster, Switzerland) (supplementary Video material in [45]). Meloxicam (1 mg/kg, Boehringer Ingelheim Basel, Switzerland) was administered s.c. at the end of surgery for continuous analgesia.

2.5. Surgery

The anaesthetized animals were positioned in sternal recumbence. Epidural was clipped and disinfected with alcohol-based skin disinfection (chlorhexidine and 2% alcohol) at the

surgical site. The epidural anaesthesia was performed between cauda (Cd)-2 and Cd-3 with an aseptic technique (26G; 38mm spinal needle).

A posterior midline skin incision (length: 10 mm) over the segment of interest was performed (Cd-4-5). This followed a sharp dissection through the fascia, exposing the two posterior longitudinal tendons [51]. This step was important to protect the vessels during Kirschner (K)-wire insertion to avoid tail necrosis [51]. The surgery was then continued with blunt midline dissection between posterior longitudinal tendons to midline muscle. A sharp dissection of the muscle in the midline was performed. Then, an Ex-Fix made of polyether ether ketone (PEEK) rings was then mounted by insertion of K-wires. The identical design of the fixator was taken from the study by Martin et al. (2014) [52] using their computer-aided design (CAD) files. Insertion of two 0.8 K-wires per adjacent vertebra from left to the right with -wire drive through the Ex-Fix K-wire insertion cut-out. Lateral subfascial vessels were then visualized during K-wire insertion to avoid damage to the vessels and prevent post-operative tail necrosis [45,51,52]. The K-wires were then cut-off with sharp pliers at the level of the ring external fixator (Figure 1) [45]. For discectomy, the anulus fibrosis of the IVD was removed sharply from the endplates of the adjacent vertebrae. Nucleus pulposus material was then removed with a Kerrison rongeur, and the endplate cartilage was debrided with a small, sharp curette (Figure 1). Then, cylindrical-shaped βTCP carriers 5 mm in ⌀ and 2 mm in height were inserted into the disc niche. The filled-in "press-fit" βTCP served as a "cage" and was compressed between the two vertebrae using the external ring fixator by fitting the threaded rods in a "press-fit" design. The skin incision was then closed s.c. using 4.0 vycril and cutaneously with 5.0 Ethilon™ (Ethicon, Johnson & Johnson, ltd., Allschwil, Switzerland), and sterile dressing was then applied. The sutures were removed after ten days post-operatively, no anaesthesia was required.

2.6. Post-Analgesia

Animals were allowed to recover until fully awake and warmth and O_2 was provided as needed. Buprenorphine analgesia (Streuli Pharma SA, Uznach, Switzerland) was continued in the first 24h post-op in drinking water (1mg/kg; 6 ml Temgesic® (Buprenorphine 0.3 mg/ml) and 360 ml drinking water and 10 ml of 5% Glucose) and with Meloxicam® 1 mg/kg (Sintetica S.A., Mendrisio, Switzerland) for four to seven days (one injection or oral application per day).

2.7. 2D digital X-rays

For all groups, true lateral and oblique anteroposterior X-rays of the surgical area were obtained immediately post-operatively to confirm correct placement of the carrier and K-wires and at six weeks and twelve weeks post-operatively to assess spinal fusion. These were collected using a digital X-ray system with 10s exposure time and 25kV (MX-20, Faxitron X-Ray Corporation, Edimex, Le Plessis, France). Post-operative and six weeks X-rays were taken in anaesthesia, and X-rays at twelve weeks were taken after sacrifice and hence did not need separate anaesthesia. The X-rays were taken at 25 kV and 10s exposure. For the X-ray at six weeks, rats were anaesthetized according to a balanced anaesthetic protocol (Fentanyl 0.005 mg/kg and Medetomidine 0.15 mg/kg and Midazolam 2 mg/kg) mixed in the same syringe and administered s.c. After s.c. injection of the anaesthetic mix, the rats were placed in a clean box and provided O_2 until loss of consciousness ensued (~ 5-10 min). After imaging the rats, the anaesthesia was reversed with a mix of Naloxone 0.12 mg/kg and Atipamezol 0.75 mg/kg and Flumazenil 0.2 mg/kg s.c. Animals recovered in clean cages until fully awake, and warmth was provided as needed. In all treatment groups, a tail sample of the surgical region (approx. 5 cm long, including the fusion site and the adjacent vertebrae) was collected after sacrifice. For quantification the X-rays were scored by two independent experienced spine surgeons blinded to the study groups using the Bridwell criteria for spinal fusion outcome [53].

2.8. Micro Computer Tomography (µCT) Analysis

µCT was performed on 70% ethanol fixed samples after overnight fixation in 4% buffered formalin. The region of interest (ROI) of the samples was then scanned with a µ-CT40 (SCANCO Medical, inc., Brüttisellen, Switzerland), using the built-in software from SCANCO Medical (SCANCO Module 64-bit; V5.15). The tails were oriented longitudinally to the axis of the X-ray beam. The X-ray tube was operated at 70 kVp and 57 mA, and the integration time was set at 300 ms with a voxel size of 10 µm. The measurements were performed perpendicular to the longitudinal axis of the caudal (Cd) vertebrae in the region of interest (ROI) between the two central screws of the fixation systems. To distinguish between soft and mineralized tissues, the tissue was segmented into two tissue types based on their greyscale (grey-level coded mineralization density), that is < 200 Hounsfield unit (HU) for soft tissues and >200 HU for mineralized tissues (βTCP carrier, mineralized cartilaginous

callus, woven and lamellar bone) [54]. For density and bone volume (BV) / total volume (TV) analyses, the TV was defined by manual segmentation (blinded to treatment groups), using the respective vertebral endplates of the fused segment as cranio-caudal, and the bone structure as circumferential limits. Analysis was carried out using the built-in software from SCANCO Medical (SCANCO Module 64-bit; V5.15). Carrier material resorption was quantified on native resolution DICOM exports using 3D Slicer v5.0.3 (3D Slicer project, https://www.slicer.org), including the Segment Editor and Segment Statistics modules [[55]]. For Voxel-based analysis and differentiation, carrier material and bone were segmented manually for three different samples analyzed in separate µCT scans, and average densities and standard deviations calculated. These showed congruent and consistent density distributions for all three samples and scans (means ± SD: bone density 7,938 ± 1,055 U; ceramic carrier 11,849 ± 931 U); allowing for application of a common threshold throughout all samples. Thresholds for density-based segmentation were set at 6,000 – 10,000 U for bone volume and 10,000 – 14,000 U for ceramic carrier volume, approximately equidistant and ± 2 SD ranges apart from the respective mean densities. The ROI for carrier resorption analysis were defined by manual segmentation, blinded to study groups and calibrated to a constant ratio relative to carrier size across scans [54]. Voxel counts for both segments (bone volume (BV) and carrier volume (CV)) were divided for each sample individually.

Evaluation and semi-quantitative scoring of the X-ray and µCT images was done independently by experienced spine surgeons, blinded to the study groups. µCT images were viewed using the OsiriX image viewer (Pixmeo SARL, Bernex, Switzerland) and scored on an adapted version of the Bridwell criteria, as previously defined and detailed in the established standard operational protocol (SOP) by Oswald *et al.* (2021) [45].

2.9. Histology

After µCT scanning, tail samples were embedded in polymethylmethacrylate (PMMA, i.e., a mixture of methyl methacrylate, cat.# 55909 and Dibutyl Phthalate cat. # 524980 (both from Sigma-Aldrich, inc., Buchs, Switzerland, and Perkadox 16 – cat. # G425.0100 Grogg Chemie, AG, Stettlen-Deisswil, Switzerland). Upon hardening (four-six weeks), the embedded tissue blocks were cut sagitally into approximately 600 µm thick ground sections using a slow-speed diamond saw (Varicut® VC50, Leco, St. Joseph, Mi, US) [56]. After mounting on acrylic glass slabs, the sections were ground and polished to a final thickness of ~150 µm (KnuthRotor-3, Struers, S.A.S. Champigny sur Marne, Cedex, France) and surface-

stained with basic fuchsin and toluidine blue/McNeal [56,57]. All histology slides were subsequently digitalized by microphotography using a Keyence VHX-6000 microscope with an automated stage (Keyence International, inc., Urdorf, Switzerland). Two to three digitalized slides per animal were scored by three independent raters, blinded to treatment groups, and rated regarding fusion success using a semi-quantitative score based on Emery *et al.* [58] and adapted to our animal model, see Table 1 and supplementary online figure S1. The 2D X-rays were rated by two blinded experienced spine surgeons.

2.10. Statistical analysis

The number of animals per group was deemed to be sufficient based on a priori power analysis. Assuming an effective size difference of 0.75 and a power of 0.80, N = 5 per group was considered a suitable sample size [59]. The data were analyzed using R 4.3.2 and GraphPad/Prism v10.0.0 for Mac OS X statistical analysis software, using the Kruskal-Wallis test for non-parametric data with Dunn's post-hoc analysis. A p-value <0.05 was considered statistically significant.

3. Results

3.1. X-ray data

The data of the X-rays showed a clear trend that groups with high dose of BMP2 had a very low spinal fusion Bridwell score showing strong spinal fusion, Fig. 2 first row and Fig. 3 (supplementary online figure S2). Mixtures of low dose BMP2 with 1 and 5 µg L51P showed equally good spinal fusion scores as with high-dose BMP2 (Fig. 3a).

3.2. µCT analysis

The bone volume (BV) relative to ceramics volume (CV) (*i.e.*, BV/CV) revealed a clear up-regulation of the ratio in favour of more bone volume relative to the remaining CV when comparing material control (PBS) with addition of BMP2 in high doses (PBS vs 10 µg BMP2, $P = 0.0074$, see Fig. 4), and if compared to all three mixtures of BMP2 with L51P, i.e., all with $P \sim 0.01$, see Fig. 4). The quantification furthermore revealed the highest ratio towards bone if the mixture of 1 µg BMP2 and 1µg of L51P was used (Figs 2 and 3b). Interestingly, L51P alone did not have a significant effect compared to PBS control (Figure 2 middle row, and Fig. 3b).

BV relative to total volume (TV), *i.e.*, BV/TV analysis did not reveal significant differences between the study groups regarding bone volume, total volume or BV/TV ratio. Mineral

density was found to be similar across groups, with no statistically discernible differences at a mean across all specimens of 2.34 ± 0.13 cm^{-1}.

3.3. Histology

Histological analysis confirmed the results derived from X-ray and µCT analysis. The images showed clear and robust ossification in samples with 10 µg BMP2, whereas almost no fusion was observed in the PBS control. Low-dose BMP2 exhibited an increased ossification with partial bridging in some cases. Interestingly, mixtures of low-dose BMP2 and L51P showed similar ossification to high-dose BMP2, even for the lowest concentration of L51P added (Fig. 3c).

Inter-rater reliability, evaluated using Cohen's weighted kappa, yielded a kappa of 0.736 (SE = 0.027, z = 13.59, p < 0.001), indicating a strong agreement. Intra-rater reliability (assessed between two timepoints, three weeks apart) showed a kappa of 0.869 (SE = 0.046, z = 8.68, < 0.01), indicating a very strong agreement.

Ordinal logistic regression analysis did not show a significant influence of sex on the outcome of histology scores (coefficient = 1.18, SE = 0.81, t = 1.50) - suggesting a minimal to non-existent effect, especially considering the relative effect sizes of treatment groups (ranges: coefficients = 19.7 - 30.1, SE = 0.99 - 1.19, *t* = 16.2 - 24.7).

3.4. Complications

In total, 60 rats were operated on. Of these, 14 rats needed to be euthanized due to complications. These complications were tail necroses (six rats, 13.0 %), open wound bites (five animals, 10.8 %), damaged/non-functional Ex-Fix (%), and other reasons (such as sudden death, and one case of a defecation problem, a total of three animals, 6.5 %). These rats were generally lost within the first five days of post-analgesic monitoring (Table 1).

4. Discussion

Unsuccessful spinal fusion, despite application of supra-physiological doses of BMP2, is a major problem in orthopaedic research [60,61]. Our results demonstrate through X-ray, µCT, and histology (Figs 2-3) that applying a mixture of BMP2 and the BMP2-analogue L51P is sufficient to reduce the required dose of BMP2 without losing ossification benefits. A lower dose of BMP2 could help to reduce the frequent side effects encountered from high-dose BMP application, particularly in spinal fusion surgeries [24-29].

This study is the first to confirm that mixtures of BMP2 and L51P were highly efficient in reducing the doses of BMP2 in a spinal fusion model and these results are in line with those

previously reported [30,36-39,62]. Previous cell cultures of mouse calvaria osteoblasts could demonstrate the interaction between BMP2 doses, the equimolar addition of Noggin (a prominent BMP2 inhibitor) and the anti-blocking effect of L51P [37,38]. Previous animal models such as an ovariectomized (OVX) rat model and long bone fracture model, it was the first time reported that mixtures of 1 µg BMP2 with 10 µg of L51P (Figures 3 and 4 of [35]). Tekari *et al.* (2017) [30] could demonstrate the inhibitory effects released by IVD cells onto MSCs in allogenic co-cultures. L51P was able to deblock these inhibitory effects of the conditioned medium released by the IVD cells [30]. As what concerns the cyto-toxicity, we have shown that exposure of higher concentrations of L51P to IVD cells had no toxic or adverse effects [62]; however, it even stimulated an enhanced IVD phenotype significantly in annulus fibrosus cells (AFC) and cartilaginous endplate cells (CEPC) in terms of proteoglycan production. When L51P was applied in a mixture of 10:1 together with BMP2 to a critical bone defect model in ovariectomized rats, the µCT and the histological sections showed very strong and complete ossification results with the exact same βTCP carrier material [35].

It is evident that the addition of L51P to BMP2 treatment accelerates and improves ossification with a lower concentration of BMP2. Further improvements could be made using smart biomaterials that allow slow growth factor release. Recent research involved alternate strategies to improve BMP2 treatment on the side of the biomaterial: in a large animal porcine model using low dose BMP2 but “fine-tuning” the carrier using for instance polyelectrolyte complex (PEC) carrier [63]. Also, in a similar rat-tail model, as presented here, a novel composite combining hydroxyapatite, βTCP phosphate microsphere/poloxamer hydrogel, in combination with BMP2 has been recently tested for improved spinal fusion [64]. Mixing BMP2 with biological add-ons like platelet rich plasma (PRP) or conditioned medium from MSCs had a moderate improvement effect in a mouse femoral bone defect with Ex-Fix model [65]. Such methods in combination with our L51P/BMP2 mixtures might improve the outcomes even further [66].

Previous investigations demonstrate the potential of L51P and βTCP for improved bone healing in a critical fracture healing model and C57Bl/6J mice [37,49].

This study forwent biomechanical testing of the fused segment. Segments were used for µCT analysis and histology, thus two-point bending or three-point bending failure tests of the fused tail segments to quantify the strength of the fused segments and to judge the bone quality of the newly formed bone were not performed. Biomechanical testing in the study

design would have resulted in a significantly higher number of animals. To comply with the 3R principles, these tests were not performed.

Additionally, the application of the PEEK-Ex-Fix was not guided by strain or force measurements, and instead controlled by surgical experience of two fellowship-trained spine surgeons and a manual "press-fit" design. Future designs would benefit from including a force-control on the threat of the "press-fit" fixator. The same Ex-Fix system was used in males and females alike, and could possibly benefit from size adjustment, as females were slightly smaller than males. The same design and dimensions of the Ex-Fix have been successfully used in disc-like angle-ply structures (DAPS) in combination with hydrogels for the regeneration of artificial IVD segments [52]. Another, question would be whether these very clear results would have been received without press-fit compression of an Ex-Fix device. We have not tested this and should be evaluated in any future experimental design. It most likely also would have caused less euthanasia due to complications like tail necroses. However, the loss of animals was significantly reduced from the start to the end of the experimental procedures because of the routine of the improved surgery procedure and with an established standard operational protocol (SOP) in place, according to the rules of the 3Rs [45].

The βTCPs were all the same size and diameter, whereas rats naturally differ in size and weight. A possible approach to allow for these differences could be "personalized", 3D-printed constructs [67]. However, the current manufacturing process of the βTCP implants did not allow for this, and the consistent carrier size allowed for standardized analysis. Future studies could also be improved through implantation of a slow growth factor release system using micro-beads or a similar hydrogel system. The current version of βTCP carrier produces a burst-release of the cytokines within two to four days as has been previously demonstrated [46].

The BMP2 analogue L51P has now been repeatedly reported to be non-cytotoxic and to induce osteogenesis with low doses of BMP2 [30,35-39,62]. Effects at other organs in the rat's body were not investigated in this study. However, additional histology would have been useful to analyze possible adverse effects in the liver and kidney. Nevertheless, the tail is relatively isolated from the rest of the body and cytokine delivery was localized, thus adverse effects in other organs are unlikely. Finally, osteogenesis could be further fine-tuned by combinations of different doses of BMP2, L51P and vascular endothelial growth factor (VEGF) [46,68].

List of Abbreviations

BMP2: Bone morphogenic protein 2

BMP2R: Bone morphogenic protein receptor

BV/CV: Bone volume relative to ceramics volume

BV/TV: Bone volume relative to total volume

βTCP: β tri-calcium phosphate

DAN: Differential screening-selected gene aberrative in neuroblastoma

MSC: Mesenchymal stem cells

L51P: BMP2 analogue - leucine replaced by proline at position 51

K-wire: Kirschner wire

Ex-Fix: External fixator

PEEK: Polyether ether ketone

PEC: Polyelectrolyte complex

PMMA: Poly methy acrylate

PRP: Platelet-rich plasma

s.c.: Subcuntaniously

SOP: Standard operational protocol

VEGF: Vascular endothelial growth factor

Acknowledgements/Funding Statement

We thank Prof. em. Walter Sebald and Prof. Dr. Thomas Müller of the Julius von Sachs Institute of the University of Würzburg, Germany, for providing the BMP2 and the BMP2 analogue L51. The βTCP carriers were kindly produced by the group of Prof. Marc Bohner of the Robert Matthys Foundation. We thank Urs Rohrer and his team for the production of the PEEK Ex-Fix and the customized extra-small hex wrench. We thank the team of Stryker Osteonics SA, Biberist, for providing the drill to perform the Kirschner wire fixations. We are grateful to Andrea Oberli, Inga Grigaitiene and Thuy-Trang Nguyen for preparation of the coated βTCP carriers and assistance in calcified tissue histology. We thank Prof. em. Willy Hofstetter and Prof. Nikola Saulacic for scientific inputs. We thank the animal care keepers and the entire veterinarian team of the centralized animal facility (CAF) of the medical faculty of the University of Bern for the continuous support. Funding was received

from the Swiss Orthopaedics Foundation (SGOT) and the clinical trials unit (CTU) of the Insel University Hospital Bern. Further support was received by the Swiss National Science Foundation (project #310030E_192674/1, https://data.snf.ch/grants/grant/192674, accessed on 22 December 2023) and by the Marie Skłodowska Curie International Training Network (ITN) "disc4all" (https://disc4all.upf.edu, accessed on 22 December 2023) grant agreement #955735 (https://cordis.europa.eu/project/id/955735, accessed on 22 December 2023), and by the Robert Mathys Foundation, grant number E19_0003. We thank Katherine Briana Crump for proof-editing our manuscript.

Supplementary materials

Supplementary material associated with this article can be found, in the online version, at doi [to be inserted].

Conflict of Interest: The authors declare no conflict of interest.

Data Availability Statement: The data can be obtained from the corresponding author.

Institutional Review Board Statement: The study design followed the ARRIVE guidelines and the study protocol was approved by the cantonal veterinary authorities of Bern on animal experimentation (Federal Food Safety and Veterinary Office, https://www.blv.admin.ch/, assessed on 27 December 2023) (approval#BE19/32).

CRediT Authorship Contribution Statement:

The study conception and design were proposed by C.E.A., S.F.B. and B.G. The study director of the animal permit was B.G. Further, B.G. has written the main draft of the manuscript. Histological analysis was devised and prepared by G.F.E., and scoring performed by B.G., P.B.-L and G.F.E., µCT quantitative analysis was carried out by G.F.E., X-ray and

µCT scoring by C.E.A., S.F.B., G.F.E. and K.A.C.O. G.F.E. performed the statistical analysis and produced the figures 2-5. Arts and graphics were made by B.G. K.A.C.O., S.F.B., B.G. and C.E.A. performed the surgeries, P.B-L. and A.S.C. assisted in pain scoring. F.S. performed the µCT scans and assisted in the µCT analysis. All co-authors edited and approved the manuscript. B.G. and C.E.A. acquired funding.

References

[1] M.L. Ferreira, K. de Luca, L.M. Haile, *et al*, Global, regional, and national burden of low back pain, 1990–2020, its attributable risk factors, and projections to 2050: a systematic analysis of the Global Burden of Disease Study 2021, Lancet Rheumatol 5 (6) (2023) e316-e329.

[2] S. Wieser, B. Horisberger, S. Schmidhauser, C. Eisenring, U. Brügger, A. Ruckstuhl, J. Dietrich, A.F. Mannion, A. Elfering, O. Tamcan, U. Müller, Cost of low back pain in Switzerland in 2005, Eur J Health Econ 12 (5) (2011) 455-467.

[3] T. Vos, A.D. Flaxman, M. Naghavi, *et al*, Years lived with disability (YLDs) for 1160 sequelae of 289 diseases and injuries 1990–2010: a systematic analysis for the Global Burden of Disease Study 2010, Lancet 380 (9859) (2012) 2163-2196.

[4] D. Hoy, L. March, P. Brooks, F. Blyth, A. Woolf, C. Bain, G. Williams, E. Smith, T. Vos, J. Barendregt, C. Murray, R. Burstein, R. Buchbinder, The global burden of low back pain: estimates from the Global Burden of Disease 2010 study, Ann Rheum Dis 73 (6) (2014) 968-974.

[5] R. Watkins, R. Watkins, R. Hanna, Non-union rate with stand-alone lateral lumbar interbody fusion, Medicine (Baltimore) 93 (29) (2014) e275.

[6] F. Veronesi, M. Sartori, C. Griffoni, M. Valacco, G. Tedesco, P.F. Davassi, A. Gasbarrini, M. Fini, G. Barbanti Brodano, Complications in Spinal Fusion Surgery: A Systematic Review of Clinically Used Cages, J Clin Med 11 (21) (2022) .

[7] B.I. Martin, S.K. Mirza, B.A. Comstock, D.T. Gray, W. Kreuter, R.A. Deyo, Reoperation rates following lumbar spine surgery and the influence of spinal fusion procedures, Spine 32 (3) (2007) 382-387.

[8] R. Wittenauer, L. Smith, K. Aden, Background paper 6.12 osteoarthritis, World Health Organisation (WHO) (2013) .

[9] D.S. Chun, K.C. Baker, W.K. Hsu, Lumbar pseudarthrosis: a review of current diagnosis and treatment, Neurosurg Focus 39 (4) (2015) E10.

[10] S.S. Rajaee, H.W. Bae, L.E. Kanim, R.B. Delamarter, Spinal fusion in the United States: analysis of trends from 1998 to 2008, Spine 37 (1) (2012) 67-76.

[11] S.E. Broida, K. Murakami, A. Abedi, H.J. Meisel, P. Hsieh, J. Wang, A. Jain, Z. Buser, S.T. Yoon, AO Spine Knowledge Forum Degenerative, Clinical risk factors associated with the development of adjacent segment disease in patients undergoing ACDF: A systematic review, Spine J 23 (1) (2023) 146-156.

[12] A. Matsugaki, M. Ito, Y. Kobayashi, T. Matsuzaka, R. Ozasa, T. Ishimoto, H. Takahashi, R. Watanabe, T. Inoue, K. Yokota, Y. Nakashima, T. Kaito, S. Okada, T. Hanawa, Y. Matsuyama, M. Matsumoto, H. Taneichi, T. Nakano, Innovative design of bone quality-targeted intervertebral spacer: accelerated functional fusion guiding

oriented collagen and apatite microstructure without autologous bone graft, Spine J 23 (4) (2023) 609-620.
[13] E.N. Phan, W.K. Hsu, Novel Approaches Guiding the Future of Spinal Biologics for Bone Regeneration, Curr Rev Musculoskelet Med 15 (3) (2022) 205-212.
[14] N. Wakao, Y. Sakai, T. Watanabe, N. Osada, T. Sugiura, H. Iida, Y. Ozawa, K. Murotani, Spinal pseudoarthrosis following osteoporotic vertebral fracture: prevalence, risk factors, and influence on patients' activities of daily living 1 year after injury, Arch Osteoporos 18 (1) (2023) 45.
[15] M.R. Urist, Bone: formation by autoinduction, Science 150 (3698) (1965) 893-899.
[16] L. Fernandez, A. Petrizzo, The Use of Bone Morphogenetic Protein 2 (BMP-2) in Spine Surgery Is It Valuable? Bull Hosp Jt Dis (2013) 81 (1) (2023) 40-45.
[17] M. D'Souza, N.A. Macdonald, J.L. Gendreau, P.J. Duddleston, A.Y. Feng, A.L. Ho, Graft Materials and Biologics for Spinal Interbody Fusion, Biomedicines 7 (4) (2019) .
[18] R.D. May, D.A. Frauchiger, C.E. Albers, A. Tekari, L.M. Benneker, F.M. Klenke, W. Hofstetter, B. Gantenbein, Application of Cytokines of the Bone Morphogenetic Protein (BMP) Family in Spinal Fusion - Effects on the Bone, Intervertebral Discs, and Mesenchymal Stromal Cells, Curr Stem Cell Res Ther 14 (8) (2019) 618-643.
[19] K.J. Song, B.W. Choi, G.H. Kim, J.H. Song, Usefulness of polyetheretherketone (PEEK) cage with plate augmentation for anterior arthrodesis in traumatic cervical spine injury, Spine J 10 (1) (2010) 50-57.
[20] K.J. Song, B.W. Choi, G.H. Kim, J.H. Song, Usefulness of polyetheretherketone (PEEK) cage with plate augmentation for anterior arthrodesis in traumatic cervical spine injury, Spine J 10 (1) (2010) 50-57.
[21] A.M. Beschloss, C.M. DiCindio, J.S. Lombardi, J.N. Shillingford, J.L. Laratta, B. Holderread, P. Louie, A.J. Pugely, Z. Sardar, A.S. Khalsa, V.M. Arlet, C. Saifi, The Rise and Fall of Bone Morphogenetic Protein 2 Throughout the United States, Clin Spine Surg 35 (6) (2022) 264-269.
[22] D. Kok, C.M.M. Peeters, Z. Mardina, D.L.M. Oterdoom, S.K. Bulstra, A.G. Veldhuizen, R. Kuijer, F.H. Wapstra, Is remaining intervertebral disc tissue interfering with bone generation during fusion of two vertebrae? PLoS ONE 14 (4) (2019) e0215536.
[23] S.C. Chan, A. Tekari, L.M. Benneker, P.F. Heini, B. Gantenbein, Osteogenic differentiation of bone marrow stromal cells is hindered by the presence of intervertebral disc cells, Arthritis Res Ther 18 (1) (2015) 29.
[24] A.W. James, G. LaChaud, J. Shen, G. Asatrian, V. Nguyen, X. Zhang, K. Ting, C. Soo, A Review of the Clinical Side Effects of Bone Morphogenetic Protein-2, Tissue Eng Part B Rev 22 (4) (2016) 284-297.
[25] M.C. Simmonds, J.V. Brown, M.K. Heirs, J.P. Higgins, R.J. Mannion, M.A. Rodgers, L.A. Stewart, Safety and Effectiveness of Recombinant Human Bone Morphogenetic Protein-2 for Spinal Fusion: A Meta-analysis of Individual-Participant Data, Ann Intern Med 158 (12) (2013) 877-889.
[26] E.J. Carragee, E.L. Hurwitz, B.K. Weiner, A critical review of recombinant human bone morphogenetic protein-2 trials in spinal surgery: emerging safety concerns and lessons learned, Spine J 11 (6) (2011) 471-491.
[27] F.A. De Stefano, T. Elarjani, J.D. Burks, S.S. Burks, A.D. Levi, Dose Adjustment Associated Complications of Bone Morphogenetic Protein: A Longitudinal Assessment, World Neurosurg 156 (2021) e64-e71.
[28] E. Argintar, S. Edwards, J. Delahay, Bone morphogenetic proteins in orthopaedic trauma surgery, Injury 42 (8) (2011) 730-734.
[29] J.N. Zara, R.K. Siu, X. Zhang, J. Shen, R. Ngo, M. Lee, W. Li, M. Chiang, J. Chung, J. Kwak, B.M. Wu, K. Ting, C. Soo, High doses of bone morphogenetic protein 2 induce

structurally abnormal bone and inflammation in vivo, Tissue Eng Part A 17 (9-10) (2011) 1389-1399.
[30] A. Tekari, R.D. May, D.A. Frauchiger, S.C.W. Chan, L.M. Benneker, B. Gantenbein, The BMP2 variant L51P restores the osteogenic differentiation of human mesenchymal stromal cells in the presence of intervertebral disc cells , Eur Cell Mater 33 (2017) 197-210.
[31] R.D. May, D.A. Frauchiger, C.E. Albers, L.M. Benneker, S. Kohl, B. Gantenbein, Inhibitory Effects of Human Primary Intervertebral Disc Cells on Human Primary Osteoblasts in a Co-Culture System, Int J Mol Sci 19 (4) (2018) .
[32] T. Makino, H. Tsukazaki, Y. Ukon, D. Tateiwa, H. Yoshikawa, T. Kaito, The Biological Enhancement of Spinal Fusion for Spinal Degenerative Disease, Int J Mol Sci 19 (8) (2018) .
[33] S.J. Brown, S.A. Turner, B.S. Balain, N.T. Davidson, S. Roberts, Is Osteogenic Differentiation of Human Nucleus Pulposus Cells a Possibility for Biological Spinal Fusion? Cartilage (2018) 1947603518754628.
[34] S. Keller, J. Nickel, J.-L. Zhang, W. Sebald, T.D. Mueller, Molecular recognition of BMP-2 and BMP receptor IA, Nat Struct Mol Biol 11 (5) (2004) 481.
[35] M. Hauser, M. Siegrist, A. Denzer, N. Saulacic, J. Grosjean, M. Bohner, W. Hofstetter, Bisphosphonates reduce biomaterial turnover in healing of critical-size rat femoral defects, J Orthop Surg (Hong Kong) 26 (3) (2018) 2309499018802487.
[36] H.M. Khattab, M. Ono, W. Sonoyama, Y. Oida, S. Shinkawa, Y. Yoshioka, K. Maekawa, Y. Tabata, K. Sugama, W. Sebald, T. Kuboki, The BMP2 antagonist inhibitor L51P enhances the osteogenic potential of BMP2 by simultaneous and delayed synergism, Bone 69 (2014) 165-173.
[37] H.J. Sebald, F.M. Klenke, M. Siegrist, C.E. Albers, W. Sebald, W. Hofstetter, Inhibition of endogenous antagonists with an engineered BMP-2 variant increases BMP-2 efficacy in rat femoral defect healing, Acta Biomater 8 (10) (2012) 3816-3820.
[38] C.E. Albers, W. Hofstetter, H.J. Sebald, W. Sebald, K.A. Siebenrock, F.M. Klenke, L51P - A BMP2 variant with osteoinductive activity via inhibition of Noggin, Bone 51 (3) (2012) 401-406.
[39] H.M. Khattab, S. Kubota, M. Takigawa, T. Kuboki, W. Sebald, The BMP-2 mutant L51P: a BMP receptor IA binding-deficient inhibitor of noggin, J Bone Miner Metab (2018) .
[40] A. Parajón, M. Alimi, R. Navarro-Ramirez, P. Christos, J.M. Torres-Campa, Y. Moriguchi, G. Lang, R. Härtl, Minimally Invasive Transforaminal Lumbar Interbody Fusion: Meta-analysis of the Fusion Rates. What is the Optimal Graft Material? Neurosurgery 81 (6) (2017) 958-971.
[41] I.H. Drespe, G.K. Polzhofer, A.S. Turner, J.N. Grauer, Animal models for spinal fusion, Spine J 5 (6 Suppl) (2005) 209S-216S.
[42] A. Tanaka, T. Shimizu, T. Kawai, S. Fujibayashi, K. Murata, S. Matsuda, B. Otsuki, Risk of further surgery after decompression in patients with diffuse idiopathic skeletal hyperostosis extending to the lumbar segments: focus on the number of residual lumbar/lumbosacral and sacroiliac mobile segments, Eur Spine J 32 (7) (2023) 2336-2343.
[43] P. Sengupta, The Laboratory Rat: Relating Its Age With Human's, Int J Prev Med 4 (6) (2013) 624-630.
[44] R. Quinn, Comparing rat's to human's age: how old is my rat in people years? Nutrition 21 (6) (2005) 775-777.

[45] K.A.C. Oswald, S.F. Bigdon, A.S. Croft, P. Bermudez-Lekerika, A. Bergadano, B. Gantenbein, C.E. Albers, Establishment of a Novel Method for Spinal Discectomy Surgery in Elderly Rats in an In Vivo Spinal Fusion Model, Meth & Prot 4 (4) (2021) .
[46] E. Wernike, W. Hofstetter, Y. Liu, G. Wu, H.J. Sebald, D. Wismeijer, E.B. Hunziker, K.A. Siebenrock, F.M. Klenke, Long-term cell-mediated protein release from calcium phosphate ceramics, J Biomed Mater Res A 92 (2) (2010) 463-474.
[47] R. Ruppert, E. Hoffmann, W. Sebald, Human bone morphogenetic protein 2 contains a heparin-binding site which modifies its biological activity, Eur J Biochem 237 (1) (1996) 295-302.
[48] T. Kirsch, J. Nickel, W. Sebald, Isolation of recombinant BMP receptor IA ectodomain and its 2:1 complex with BMP-2, FEBS Lett 468 (2-3) (2000) 215-219.
[49] M. Hauser, M. Siegrist, I. Keller, W. Hofstetter, Healing of fractures in osteoporotic bones in mice treated with bisphosphonates - A transcriptome analysis, Bone 112 (2018) 107-119.
[50] E. Wernike, M.O. Montjovent, Y. Liu, D. Wismeijer, E.B. Hunziker, K.A. Siebenrock, W. Hofstetter, F.M. Klenke, VEGF incorporated into calcium phosphate ceramics promotes vascularisation and bone formation in vivo, Eur Cell Mater 19 (2010) 30-40.
[51] H. Gebhard, A.R. James, R.D. Bowles, J.P. Dyke, T. Saleh, S.P. Doty, L.J. Bonassar, R. Härtl, Biological intervertebral disc replacement: an in vivo model and comparison of two surgical techniques to approach the rat caudal disc, Evid Based Spine Care J 2 (1) (2011) 29-35.
[52] J.T. Martin, A.H. Milby, J.A. Chiaro, D.H. Kim, N.M. Hebela, L.J. Smith, D.M. Elliott, R.L. Mauck, Translation of an engineered nanofibrous disc-like angle-ply structure for intervertebral disc replacement in a small animal model, Acta Biomater 10 (6) (2014) 2473-2481.
[53] K.H. Bridwell, L.G. Lenke, K.W. McEnery, C. Baldus, K. Blanke, Anterior fresh frozen structural allografts in the thoracic and lumbar spine. Do they work if combined with posterior fusion and instrumentation in adult patients with kyphosis or anterior column defects? Spine 20 (12) (1995) 1410-1418.
[54] M.L. Bouxsein, S.K. Boyd, B.A. Christiansen, R.E. Guldberg, K.J. Jepsen, R. Müller, Guidelines for assessment of bone microstructure in rodents using micro-computed tomography, J Bone Miner Res 25 (7) (2010) 1468-1486.
[55] R.P. Kikinis, S.D. Vosburgh, K. Kirby, 3D Slicer: A Platform for Subject-Specific Image Analysis, Visualization, and Clinical Support. F.A. JoleszIntraoperative Imaging and Image-Guided Therapy. Springer New York, 2014, pp. 277-289.
[56] N.P. Lang, J.-C. Imber, K.N. Lang, B. Schmid, F. Muñoz, D.D. Bosshardt, N. Saulacic, Sequential osseointegration of a novel implant system based on 3D printing in comparison with conventional titanium implants, Clin Oral Implants Res (2023) .
[57] M.A. Abreu, L.G. Baroza, M.A. Rossi, Toluidine Blue-Basic Fuchsin Stain for Glycolmethacrylate Embedded Tissue, J Histotechnol (2013) 139-140.
[58] S.E. Emery, M.S. Brazinski, A. Koka, J.S. Bensusan, S. Stevenson, The biological and biomechanical effects of irradiation on anterior spinal bone grafts in a canine model, J Bone Joint Surg Am 76 (4) (1994) 540-548.
[59] F. Faul, E. Erdfelder, A.G. Lang, A. Buchner, G*Power 3: a flexible statistical power analysis program for the social, behavioral, and biomedical sciences, Behav Res Methods 39 (2) (2007) 175-191.
[60] H.Y. Choi, S.J. Hyun, C.H. Lee, J.H. Youn, M.Y. Ryu, K.J. Kim, Safety and Efficacy of Recombinant Human Bone Morphogenetic Protein-2 in Multilevel Posterolateral Lumbar Fusion in a Prospective, Randomized, Controlled Trial, Neurospine 19 (3) (2022) 838-846.

[61] E.N. Phan, W.K. Hsu, Novel Approaches Guiding the Future of Spinal Biologics for Bone Regeneration, Curr Rev Musculoskelet Med 15 (3) (2022) 205-212.
[62] R.D. May, D.A. Frauchiger, C.E. Albers, W. Hofstetter, B. Gantenbein, Exogenous Stimulation of Human Intervertebral Disc Cells in 3-Dimensional Alginate Bead Culture With BMP2 and L51P: Cytocompatibility and Effects on Cell Phenotype, Neurospine 17 (1) (2020) 77-87.
[63] T. Hu, L. Liu, R.W.M. Lam, S.Y. Toh, S.A. Abbah, M. Wang, A.K. Ramruttun, K. Bhakoo, S. Cool, J. Li, J. Cho-Hong Goh, H.K. Wong, Bone marrow mesenchymal stem cells with low dose bone morphogenetic protein 2 enhances scaffold-based spinal fusion in a porcine model, J Tissue Eng Regen Med 16 (1) (2022) 63-75.
[64] D. Tateiwa, S. Nakagawa, H. Tsukazaki, R. Okada, J. Kodama, J. Kushioka, Z. Bal, Y. Ukon, H. Hirai, T. Kaito, A novel BMP-2-loaded hydroxyapatite/beta-tricalcium phosphate microsphere/hydrogel composite for bone regeneration, Sci Rep 11 (1) (2021) 16924.
[65] C. Vater, M. Hetz, M. Quade, A. Lode, M. Gelinsky, S. Rammelt, S. Zwingenberger, H. Bretschneider, Combined application of BMP-2 and naturally occurring bioactive factor mixtures for the optimized therapy of segmental bone defects, Acta Biomater 157 (2023) 162-174.
[66] H. Bretschneider, M. Quade, A. Lode, M. Gelinsky, S. Rammelt, C. Vater, Chemotactic and Angiogenic Potential of Mineralized Collagen Scaffolds Functionalized with Naturally Occurring Bioactive Factor Mixtures to Stimulate Bone Regeneration, Int J Mol Sci 22 (11) (2021) 5836.
[67] W.C. Lo, L.W. Tsai, Y.S. Yang, R.W.Y. Chan, Understanding the Future Prospects of Synergizing Minimally Invasive Transforaminal Lumbar Interbody Fusion Surgery with Ceramics and Regenerative Cellular Therapies, Int J Mol Sci 22 (7) (2021) .
[68] S. He, J. Fang, C. Zhong, M. Wang, F. Ren, Spatiotemporal Delivery of pBMP2 and pVEGF by a Core-Sheath Structured Fiber-Hydrogel Gene-Activated Matrix Loaded with Peptide-Modified Nanoparticles for Critical-Sized Bone Defect Repair, Adv Healthc Mater 11 (21) (2022) e2201096.

List of Figures

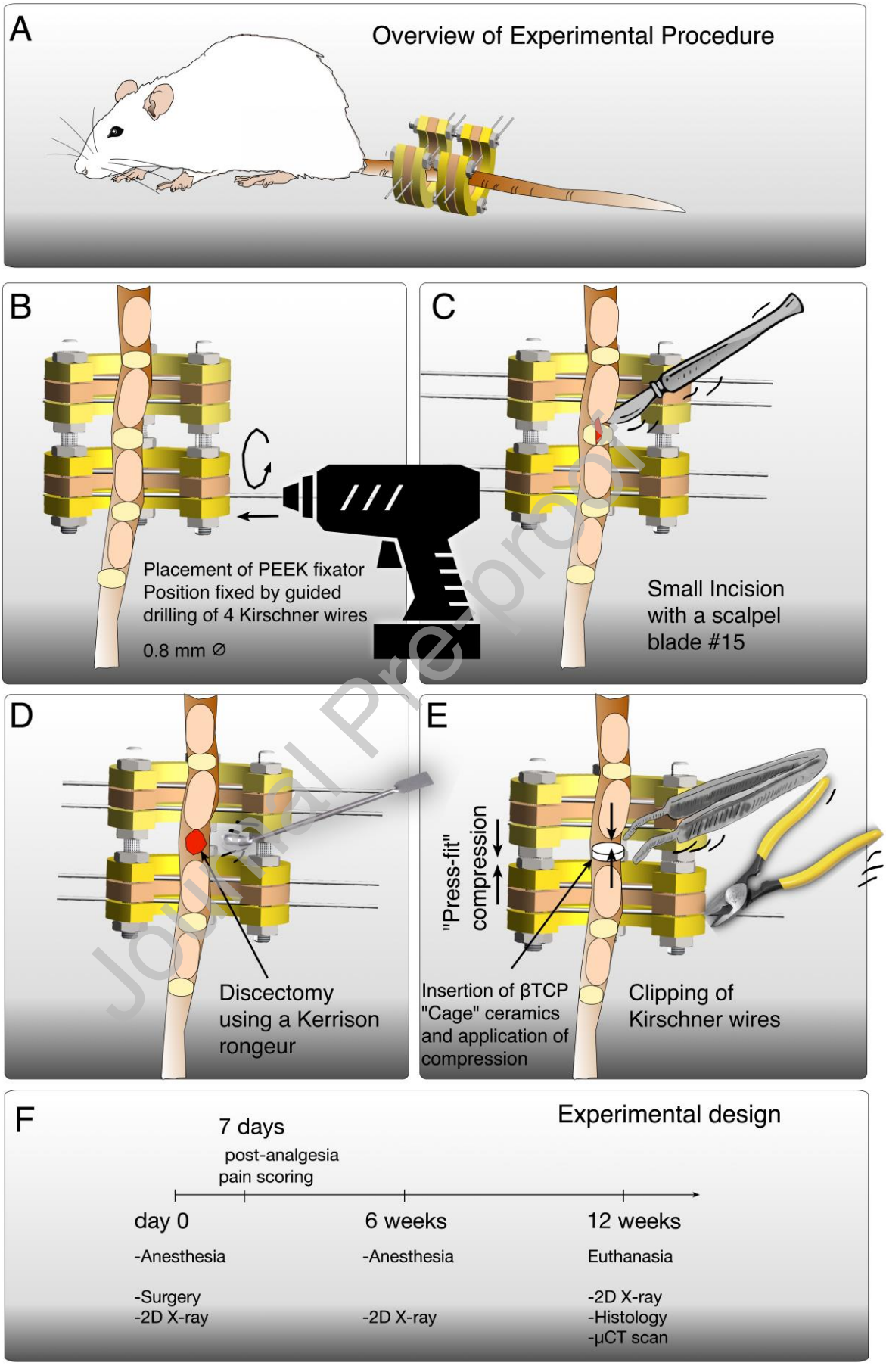

Fig. 1. Experimental Procedure. Sketch illustrating the SOP for spinal surgery in elderly rats for spinal fusion models. (a) Overview of Ex-Fix mounted on adult Wistar rat (b) Mounting of Ex-Fix by drilling four Kirschner wires through two adjacent vertebrae (c) Midline incision using a small scalpel blade, e.g. #15 (d) Discectomy with a Kerrison rongeur (e) Insertion of βTCP carrier (± coated with BMPs). This procedure was followed by press-fit compression using the Ex-Fix, finalized by a two-step-wound closure and clipping of the K-wires. (f) Experimental design of the 12-weeks post-operative follow-up and read-out parameters. Parts of the figure has been republished with permission from [45] ©CC-YY, MDPI, Basel, Switzerland.

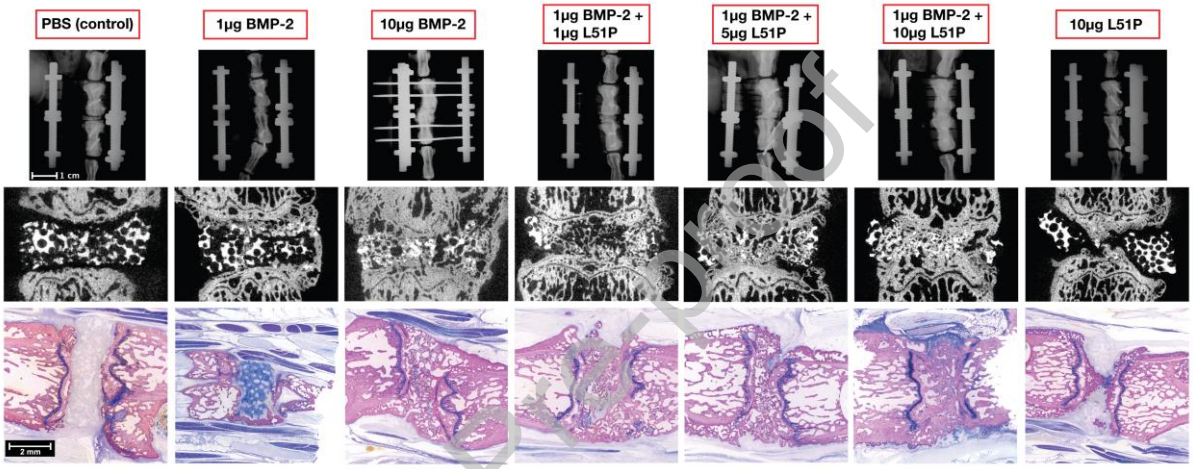

Fig. 2. Overview of the results of the proximal tail region of coccygeal spinal fusion model of elderly Wistar rats twelve weeks post-operatively, showing one representative image per 2D X-ray, apical position (Faxitron), b) Mid-sagittal plane section of µCT images, in white colour remaining βTCP carrier, in grey colour bone c) histology of PMMA-embedded thick sections (~200 µm).

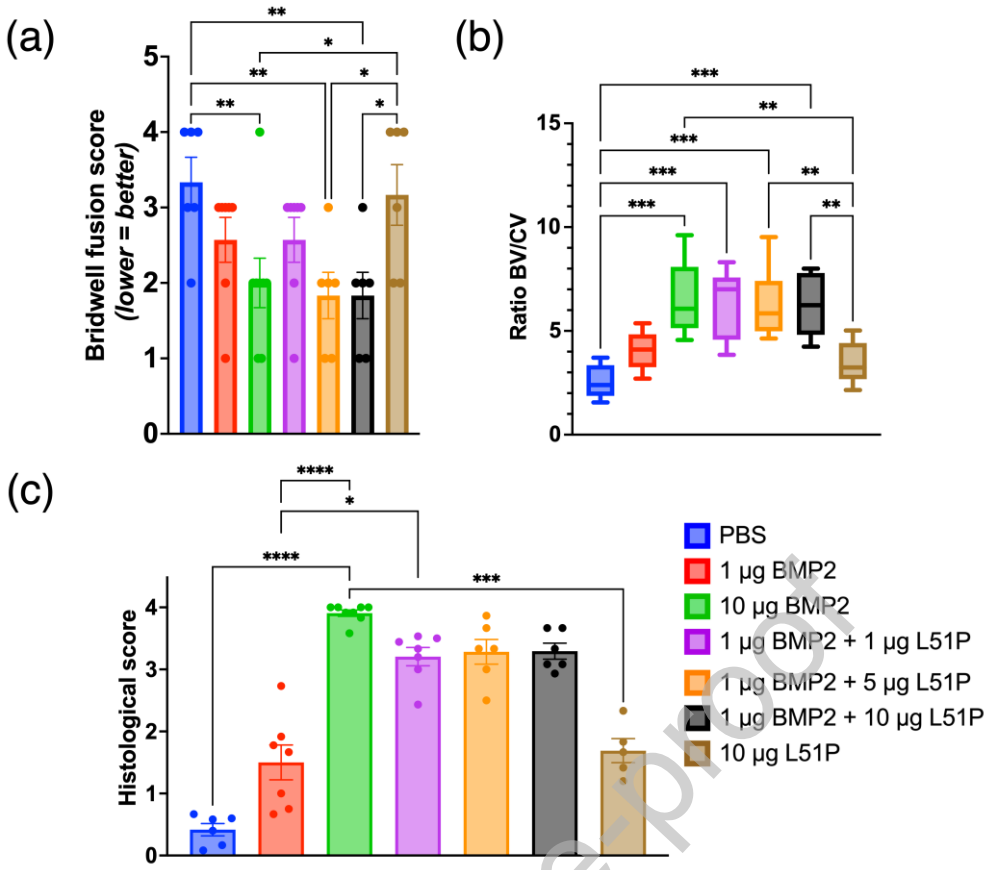

Fig. 3. A) Semi-quantitative analysis of spinal fusion model of elderly Wistar rats by Bridwell scores [53]. Two independent orthopaedic surgeons quantified the X-ray images (0 is best and 4 is worst). Shown are means ± SEM. Stars indicate level of statistical significance; *: $P < 0.05$, **: $P < 0.025$, ***: $P < 0.01$. **B)** Whisker plots of bone volume relative to ceramics volume (βTCP) (BV/CV) of µCT data. Shown are min to max and medians. Stars indicate level of statistical significance; *: $P < 0.05$, **: $P < 0.025$, ***: $P < 0.01$. **C)** Bar plots of histology scoring of PMMA-thick sections of the coccygeal spinal fusion model of elderly Wistar rat according to Emery *et al.* (1994) **[58]**. Shown are the means ± SEM of the histological scores of three independent scorers. Stars indicate level of statistical significance; *: $P < 0.05$, **: $P < 0.025$, ***: $P < 0.01$.

List of Tables

Table 1. Experimental design and sample sizes of the *in-vivo* elderly Wistar rat model. The last two columns show the lost animals due to complications per experimental group and sex.

					Lost animals	
Experimental group		male	female	Sum	male	female
1	PBS	4	4	8	2	0
2	1 µg BMP2	4	3	7	1	1
3	10 µg BMP2	3	3	6	1	0
4	1 µg BMP2 + 1 µg L51P	2	5	7	4	0
5	1 µg BMP2 + 5 µg L51P	3	3	6	1	0
6	1 µg BMP2 + 10 µg L51P	3	3	6	0	0
7	10 µg L51P	3	3	6	2	2
	Total animals	22	24	46	11	3

Table 2. The adapted histological fusion scores based on Emery *et al.* (1994) [58]

Score	Criteria
0	Carrier only, absence of bone-ingrowth
1	Partial bone-ingrowth, lacking bone bridge
2	Bone bridge present, <50% bridging bone
3	>50% bridging bone
4	Bone only

Statement of Significance

Spinal fusion surgery is frequently applied to treat spinal pathologies. Bone Morphogenic Protein-2 (BMP2) has been approved by the U .S. Food and Drug Administration (FDA-) and by the "Conformité Européenne" (CE)-label.
However, its application is expensive and high concentrations cause side-effects. This research targets the improvement of the efficacy of BMP2 in spinal fusion surgery.

Graphical Abstract

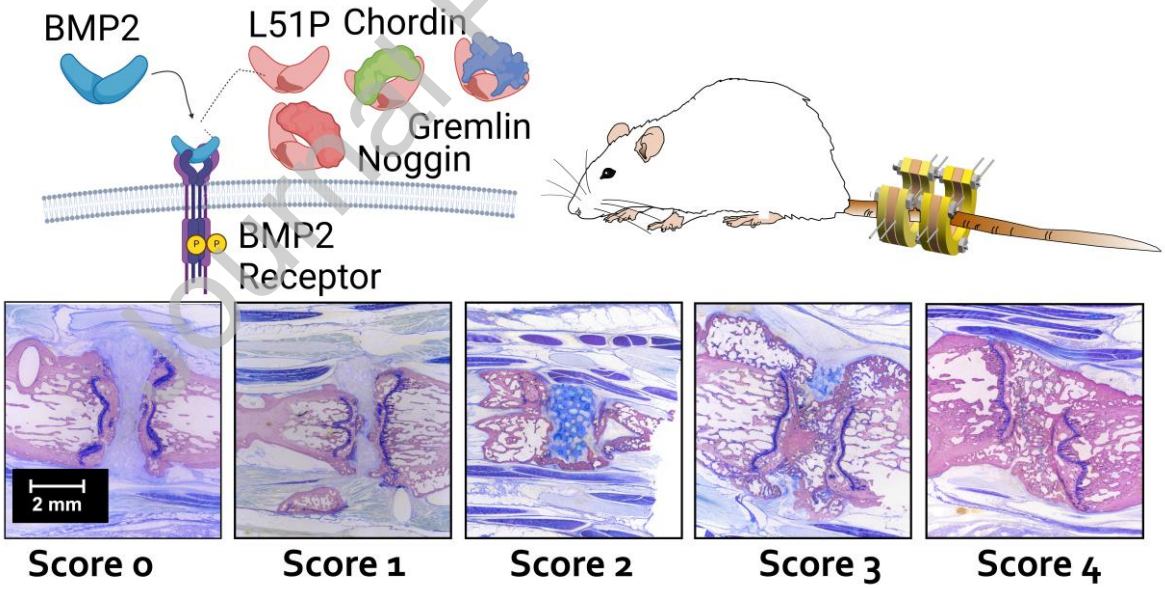

Conflict of Interest

The authors declare no conflict of interest.